# The Cu-Pr (Copper-Praseodymium) System

By P.R. Subramanian and D.E. Laughlin
Carnegie Mellon University

## Equilibrium Diagram

The equilibrium phases of the Cu-Pr system are: (1) the liquid, L, without any miscibility gaps; (2) the fcc terminal solid solution, (Cu), with negligible solid solubility of Pr in (Cu); (3) the Pr-rich bcc terminal solid solution, (βPr), based on the equilibrium phase of pure Pr between 795 and 931 °C (the solid solubility of Cu in (βPr) is negligible); (4) the Pr-rich dcph terminal solid solution, (αPr), stable below 795 °C, and with negligible solid solubility of Cu in (αPr); (5) the orthorhombic intermediate phase, $Cu_6Pr$, stable up to the congruent melting temperature of 962 °C; (6) the hexagonal phase, $Cu_5Pr$, stable up to the peritectic temperature of ~837 °C; (7) the orthorhombic phase, $Cu_4Pr$, stable up to the peritectic temperature of 824 °C; (8) the orthorhombic phase, $Cu_2Pr$, stable up to the congruent melting temperature of 841 °C; and (9) the most Pr-rich intermediate phase, CuPr, stable up to the peritectic melting temperature of 563 °C.

The present assessment of the Cu-Pr system is mainly a revision of the original phase diagram of [34Can] that was later reproduced in [Hansen]. The Pr used in the experiments of [34Can] was quite impure; [86Gsc1] estimated the purity to be <90 at.%. However, the original work is fairly complete with regard to the existence of the various intermediate phases, with the exception of the hexagonal $Cu_5Pr$ phase. The existence of $Cu_5Pr$ was noted by [61Dwi], who reported on the occurrence of $Cu_5RE$ compounds of the rare earths with the hexagonal $CaCu_5$ structure. Additionally, the two Cu-rich eutectic temperatures in the phase diagram of [34Can] are ~20 °C higher than the values obtained by interpolation of eutectic data for the other Cu-lanthanide systems (see "The Copper-Rare Earth Systems," in this issue). The assessed Cu-Pr equilibrium diagram in Fig. 1 is accepted from [34Can] with some modifications, namely, the revision of the Cu-rich eutectics based on the systematic of Cu-lanthanide systems and the inclusion of the $Cu_5Pr$ phase.

**Fig. 1 Assessed Cu-Pr Phase Diagram**

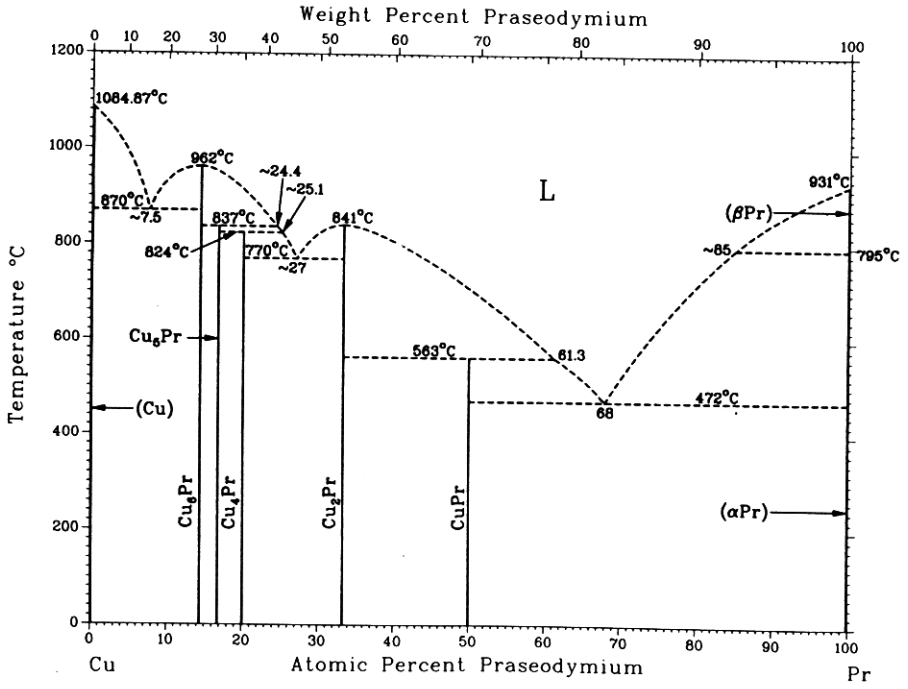


P.R. Subramanian and D.E. Laughlin, 1988.

The elemental melting points also have been adjusted to conform to the accepted values for Cu from [Melt] and for Pr from [78Bea] and [86Gsc2].

### Terminal Solid Solubility

The phase diagram of [34Can], and the subsequent compilation of [Hansen], do not indicate the existence of any terminal solid solubility in the Cu-Pr system.

### Liquidus and Solidus

Experimental data for the Cu-Pr liquidus boundaries are listed in Table 1. The melting points of (Cu) and (βPr) are accepted as 1084.87 °C [Melt] and 931 °C [78Bea, 86Gsc2], respectively. The α ↔ β transition temperature for Pr is accepted from [78Bea] and [86Gsc2] to be 795 °C.

**Table 1 Cu-Pr Experimental Liquidus Data**

| Temperature(a), °C | Composition, at.% Pr | Temperature(a), °C | Composition, at.% Pr |
|---|---|---|---|
| 1041 | 2.3 | 813 | 29.0 |
| 982 | 4.8 | 832 | 31.1 |
| 934 | 6.1 | 841 | 33.3 |
| 891 | 7.5 | 836 | 35.5 |
| 936 | 10.1 | 802 | 40.4 |
| 958 | 13.1 | 755 | 45.6 |
| 962 | 14.3 | 692 | 51.5 |
| 951 | 16.2 | 618 | 57.5 |
| 935 | 17.8 | 526 | 64.3 |
| 915 | 19.5 | 472 | 68.0 |
| 862 | 23.1 | 566 | 71.9 |
| 826 | 25.0 | 731 | 80.2 |
| 792 | 27.0 | 848 | 89.6 |

From [34Can].
(a) Liquidus temperatures are as reported in [34Can] and have not been corrected to the 1968 temperature scale (IPTS-68).

Although the effect of Cu on the α ↔ β transformation is not known [61Gsc], the invariant temperature at which the three phases, liquid, (αPr), and (βPr) coexist in equilibrium is expected to be very close to 795 °C, because the solubility of Cu in Pr at this temperature is very small. The transformation type has not been reported. However, for the Cu-Ce system (in this issue), there is experimental evidence of a catatectic reaction taking place at high temperature in the Ce-rich end, and because Cu-lanthanide systems show a systematic behavior with respect to physical properties, the α ↔ β transformation at the Pr-rich end is also expected to occur through a catatectic reaction, in concurrence with the behavior in the Cu-Ce system. This is supported further by evidence from the RE-Ag [82Gsc] and RE-Au [83Gsc] phase diagrams, both of which show catatectic reactions for the (bcc ↔ dcph) and (bcc ↔ fcc) transformations.

The initial slope at the Pr-rich end, evaluated from the van't Hoff approximation for dilute alloys, was estimated as –17 °C/at.% Cu. However, the experimental liquidus from Fig. 1 does not agree with the calculated slope and shows a deviation at fixed temperatures toward higher solute content.

The various invariant reactions occurring in the Cu-Pr system are summarized in Table 2. The present evaluators have shown that the invariant temperatures in the various Cu-lanthanide systems show a systematic variation as one progresses across the lanthanide series (see "The Copper-Rare Earth Systems," in this issue). The melting temperatures of the Cu-Pr intermediate phases fit in with this general trend observed for the Cu-lanthanide systems.

The assessed eutectic reactions in the Cu-Pr system are: (1) L ↔ (Cu) + $Cu_6Pr$ at 7.5 at.% Pr and 870 °C; (2) L ↔ $Cu_4Pr$ + $Cu_2Pr$ at 27.0 at.% Pr and 770 °C, and (3) L ↔ CuPr + (αPr) at 68.0 at.% Pr and 472 °C.

**Table 2 Special Points of the Assessed Cu-Pr Phase Diagram**

| Reaction | Compositions of the respective phases, at.% Pr | | | Temperature, °C | Reaction type | Reference |
|---|---|---|---|---|---|---|
| (Cu) ↔ L | | 0.0 | | 1084.87 | Melting point | [Melt] |
| L ↔ (Cu) + $Cu_6Pr$ | 7.5 | ~0 | 14.3 | 870 | Eutectic | (a) |
| L ↔ $Cu_6Pr$ | | 14.3 | | 962 | Congruent | [34Can] |
| L + $Cu_6Pr$ ↔ $Cu_5Pr$ | 24.4 | 14.3 | 16.7 | 837 | Peritectic | (a) |
| L + $Cu_5Pr$ ↔ $Cu_4Pr$ | 25.1 | 16.7 | 20.0 | 824 | Peritectic | [34Can] |
| L ↔ $Cu_4Pr$ + $Cu_2Pr$ | ~27.0 | 20.0 | 33.3 | 770 | Eutectic | (a) |
| L ↔ $Cu_2Pr$ | | 33.3 | | 841 | Congruent | [34Can] |
| L + $Cu_2Pr$ ↔ CuPr | 61.3 | 33.3 | 50.0 | 563 | Peritectic | [34Can] |
| L ↔ CuPr + (αPr) | 68 | 50 | ~100 | 472 | Eutectic | [34Can] |
| (βPr) ↔ L + (αPr) | ~100 | ~85 | ~100 | ~795 | Catatectic | (b) |
| (αPr) ↔ (βPr) | | 100 | | 795 | Allotropic | [78Bea, 86Gsc] |
| (βPr) ↔ L | | 100 | | 931 | Melting point | [78Bea, 86Gsc] |

(a) Invariant temperature was determined by interpolation of corresponding data for the other Cu-lanthanide systems, as given in "The Copper-Rare Earth Systems," in this issue. (b) Estimated from systematics of Cu-lanthanide systems.

**Table 3 Cu-Pr Crystal Structure Data**

| Phase | Composition, at.% Pr | Pearson symbol | Space group | Strukturbericht designation | Prototype |
|---|---|---|---|---|---|
| (Cu) | 0 | *cF*4 | $Fm\bar{3}m$ | *A*1 | Cu |
| $Cu_6Pr$ | ~14.29 | *oP*28 | *Pnma* | ... | $CeCu_6$ |
| $Cu_5Pr$ | ~16.67 | *hP*6 | *P6/mmm* | $D2_d$ | $CaCu_5$ |
| $Cu_4Pr$ | ~20.0 | *oP*20 | *Pnnm* | ... | $CeCu_4$ |
| $Cu_2Pr$ | ~33.3 | *oI*12 | *Imma* | ... | $CeCu_2$ |
| CuPr | ~50 | *oP*8 | *Pnma* | *B*27 | FeB |
| (βPr) | 100 | *cI*2 | $Im\bar{3}m$ | *A*2 | W |
| (αPr) | 100 | *hP*4 | $P6_3/mmc$ | *A*3′ | (αLa) |

**Table 4 Cu-Pr Lattice Parameter Data**

| Phase | Composition, at.% Pr | Lattice parameters, nm *a* | *b* | *c* | Comment | Reference |
|---|---|---|---|---|---|---|
| (Cu) | 0 | 0.36146 | ... | ... | At 25 °C | [Massalski] |
| $Cu_6Pr$ | ~14.29 | 0.8101 | 0.5081 | 1.0140 | ... | [70Bus] |
| $Cu_5Pr$ | ~16.67 | 0.5126 | ... | 0.4109 | ... | (a) |
| $Cu_4Pr$ | ~20.0 | 0.454 | 0.808 | 0.922 | ... | [79Pop] |
| $Cu_2Pr$ | ~33.3 | 0.4400 | 0.7024 | 0.7435 | ... | [63Sto] |
| CuPr | ~50 | 0.7343 | 0.4584 | 0.5604 | ... | [65Dwi] |
| (βPr) | 100 | 0.413 | ... | ... | At 821 °C | [78Bea, 86Gsc] |
| (αPr) | 100 | 0.36721 | ... | 1.18326 | At 24 °C | [78Bea, 86Gsc] |

(a) [61Dwi, 71Bus, 75And, 79Pop, 81And].

The assessed Cu-$Cu_6Pr$ and $Cu_4Pr$-$Cu_2Pr$ eutectic temperatures are based on systematics of Cu-lanthanide systems and are ~20 °C lower than the experimental value of [34Can]. The CuPr-(αPr) eutectic temperature is from [34Can] and is in good agreement with the general trend for the Cu-lanthanide systems.

### Intermediate Phases

The phase diagram of [34Can] shows the existence of four intermediate phases—$Cu_6Pr$, $Cu_4Pr$, $Cu_2Pr$, and CuPr—all occurring at stoichiometric compositions.

Based on X-ray examination, [61Dwi] identified the existence of $Cu_5Pr$ with the hexagonal $CaCu_5$ prototype structure. The presence of $Cu_5Pr$ is indicated in Fig. 1 by a dashed line at the stoichiometric composition of 16.67 at.% Pr. $Cu_5Pr$ is likely to form from $Cu_6Pr$ and the liquid of composition ~24.5 at.% Pr through a peritectic reaction at ~837 °C. The reaction type is consistent with that observed for alloys of Cu with the light lanthanides. Similarly, the invariant temperature has been determined by interpolation of the melting data for the other Cu-lanthanide phase with the $AB_5$ stoichiometry.

[81Blo] reported the existence of $Cu_{13}RE$ compounds with the cubic $NaZn_{13}$ structure for RE = La and Pr. These compounds, however, have been shown to exist only in splat-cooled alloys and are therefore likely to be metastable. Note that the composition of $Cu_{13}Pr$ (7.7 at.% Pr) is very close to the composition of the eutectic point at the Pr-rich end.

## Crystal Structures and Lattice Parameters

Lattice parameters, crystal structures, and related parameters for the various phases are shown in Tables 3 and 4. Data for the (αPr) and (βPr) phases are from [78Bea] and [86Gsc2].

From X-ray diffraction data, [70Bus] confirmed that $Cu_6Pr$ crystallizes with an orthorhombic $CeCu_6$ prototype structure. Their lattice parameter measurements were conducted on alloys prepared from 99.99% pure Cu and 99.9% pure Pr. $Cu_5Pr$ has a hexagonal $CaCu_5$ structure, and lattice parameters reported for this phase by [61Dwi], [71Bus], [75And], [79Pop], and [81And] are in good agreement. Although the existence of $Cu_4Pr$ was reported more than 50 years ago [34Can], the only available report of the crystal structure and lattice parameter data for $Cu_4Pr$ is by [79Pop]. $Cu_4Pr$ is reported by [79Pop] to form with an orthorhombic structure. This phase is probably isotypic with $CeCu_4$ (space group *Pnnm*, Pearson symbol *oP*20). $Cu_2Pr$ is reported by [63Sto] to form with the orthorhombic $CeCu_2$ prototype structure. The equiatomic phase, CuPr, is the most Pr-rich phase in the Cu-Pr system and crystallizes with an orthorhombic FeB structure. The lattice parameters reported for CuPr by [65Dwi] and [65Wal] are in disagreement, with the unit cell volume calculated from the data of [65Dwi] being lower than that obtained from the data of [65Wal]. For CuCe, the lattice parameter data of [65Dwi] was preferred over that of [65Wal], and therefore, in the absence of other evidence, the accepted lattice parameter data for CuPr are taken from [65Dwi],

**Fig. 2 Assessed vs Calculated Cu-Pr Phase Diagram**

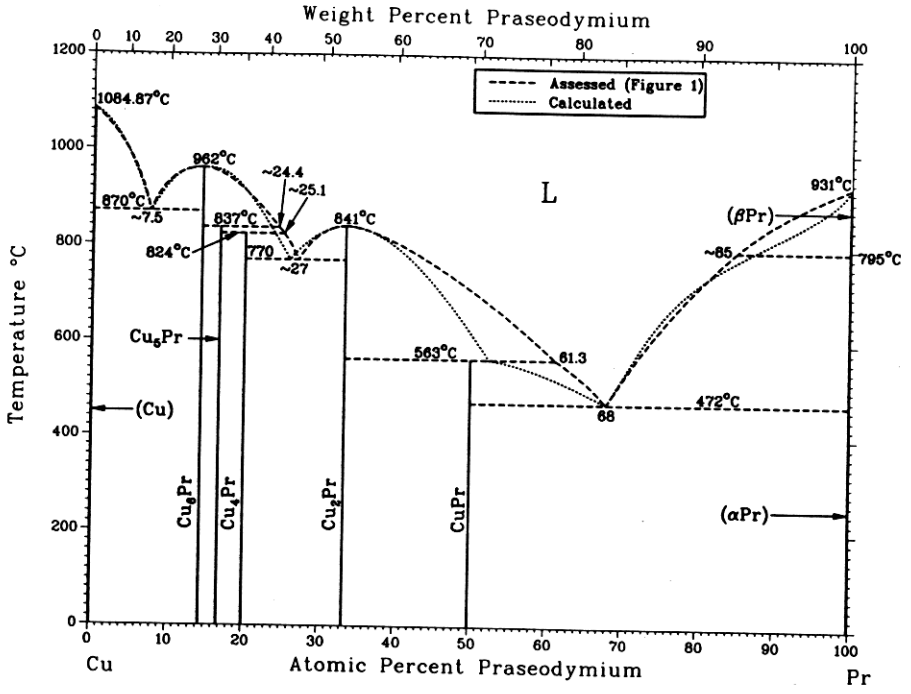


P.R. Subramanian and D.E. Laughlin, 1988.

in concurrence with the systematics of Cu-lanthanide phases.

## Thermodynamics

Experimental thermodynamic investigations on the Cu-Pr intermediate phases have so far been confined to low-temperature specific heat measurements [74Wun, 83Kwa]. These measurements have been made in the vicinity of 0 to 10 K, and as such, have no bearing on the temperature range of interest in the phase diagram.

### Thermodynamic Modeling

The following assumptions were made in the present approach:

The solid phases (Cu), (αPr), and (βPr) have no significant solid solubility.

The lattice stability parameters for the (Cu) and (βPr) phases are derived from the enthalpies of fusion, as well as the melting points, of the respective elements. The lattice stability parameters for (αPr) are derived from those of (βPr) and the temperature and enthalpy of the allotropic transformation (αPr) ↔ (βPr). The resultant expressions are given in Table 5, where pure liquid Cu and pure liquid Pr have been chosen as standard states.

- The liquid behaves like a subregular solution. The excess molar Gibbs energy of the liquid can therefore be expressed in terms of two temperature-independent parameters as follows:

$$G^{ex}(L) = X(1-X)(A + BX) \qquad \text{(Eq 1)}$$

where $X$ is the atomic fraction of Pr.

- All of the intermediate phases are line phases, i.e., the phases show nil homogeneity ranges.

The revised terminal eutectic data in Fig. 1 were utilized for deriving the following function for the integral molar excess Gibbs energy of the liquid:

$$G^{ex}(L) = X(1-X)(-149\,347 + 101\,230\,X) \qquad \text{(Eq 2)}$$

The integral molar Gibbs energies of the intermediate phases were derived from considerations of equilibrium between the liquid and the respective intermediate phases at various invariant temperatures. The Gibbs energies of the phases at various temperatures were then fitted by least-squares analysis to give the expressions listed in Table 5.

Liquidus boundaries were derived at selected temperatures from the thermodynamic functions listed in Table 5. The resultant boundaries, shown in Fig. 2, match quite well with the experimental liquidus, with some exceptions in selected regions. These are discussed in detail below.

#### 15 to 68 at.% Pr

The calculated eutectic composition at 770 °C lies at ~25.5 at.% Pr, and correspondingly, the $Cu_4Pr$ + L/L

**Table 5 Thermodynamic Properties of Cu-Pr Phases**

**Lattice stability parameters for Cu(a)**

$G^0(Cu, L) = 0$
$G^0(Cu, fcc) = -13\,054 + 9.613\,T$

**Lattice stability parameters for Pr(b)**

$G^0(Pr, L) = 0$
$G^0(Pr, bcc) = -6890 + 5.722\,T$
$G^0(Pr, dcph) = -10\,060 + 8.690\,T$

**Integral molar Gibbs energies(c)**

$G(L) = X(1-X)(-149\,347 + 101\,230\,X) + RT[X \ln X + (1-X)\ln(1-X)]$
$\Delta_f G(Cu_6Pr) = -33\,570 + 10.40\,T$
$\Delta_f G(Cu_5Pr) = -30\,681 + 6.50\,T$
$\Delta_f G(Cu_4Pr) = -27\,767 + 2.07\,T$
$\Delta_f G(Cu_2Pr) = -43\,574 + 10.76\,T$
$\Delta_f G(CuPr) = -46\,736 + 20.55\,T$

**Note:** Standard states: pure liquid Cu and pure liquid Pr. Gibbs energies are expressed in J/mol, and temperatures are in K. $X$ is the atomic fraction of Pr. Mol refers to the atom as the elementary entity.
(**a**) From [Hultgren,E]. (**b**) From [83Cha]; melting and transformation temperatures are from [78Bea] and [86Gsc]. (**c**) From the phase diagram [this work].

liquidus as well as the L/L + $Cu_2Pr$ liquidus show deviations at fixed temperatures toward higher Cu content. In addition, the liquidus composition at the peritectic temperature of 837 °C is ~23.2 at.% Pr, which is slightly lower than the interpolated value from the experimental liquidus. Similar shifts have been observed for the corresponding regions in the Cu-Ce system, thus indicating that the observed deviation in the eutectic composition is at least systematic. The calculated congruent melting temperature of $Cu_2Pr$, however, is in good accord with the experimental data. The Gibbs energy function for $Cu_2Pr$ was derived by selecting liquidus data at only two invariant temperatures (770 and 841 °C), with the exclusion of data at 563 °C. As a result, the calculated liquidus composition at the peritectic temperature of 563 °C was observed to be ~9 at.% lower than the experimental value, with a concomitant shift in the $Cu_2Pr$ + L/L liquidus toward higher Cu concentrations. Alternately, the inclusion of liquidus data at 563 °C in the Gibbs energy calculation resulted in a poorer fit, especially near the $Cu_4Pr$-$Cu_2Pr$ eutectic, with the calculated eutectic temperature being almost 25 °C higher than the accepted value. Because the $Cu_4Pr$-$Cu_2Pr$ eutectic data are more accurate than the liquidus composition at the peritectic temperature, the original Gibbs energy function for $Cu_2Pr$ as listed in Table 5 was chosen as being more consistent with the experimental data.

### 68 to 100 at.% Pr

The L/L + (αPr) liquidus is in good accord with the experimental values, with slight deviations, however, in the region close to the α ↔ β invariant temperature. At the transformation temperature of ~795 °C, the calculated liquidus corresponds to ~87.1 at.% Pr, which is higher than the interpolated value from the experimental data. Consequently, the L/L + (βPr) liquidus also shows a shift toward higher Pr content. These deviations from the experimental liquidus, however, are not very significant, if one considers that the experimental liquidus was constructed from only three data points. Moreover, the α ↔ β allotropic transformation is not reported in the experimental investigation of [34Can], from whose data the experimental liquidus was derived. In conclusion, the parameters listed in Table 5 were deemed to provide the best possible match between the experimental phase boundaries and the calculated liquidus.

**Table 6 Calculated Enthalpies of Formation of Cu-Pr Intermediate Phases vs Theoretical Estimates Based on Miedema's Model.**

| Phase | Enthalpy of formation, kJ/mol: Present modeling | Miedema model(a) |
|---|---|---|
| $Cu_6Pr$ | –33.6 | –28.8 |
| $Cu_5Pr$ | –30.7 | –31.3 |
| $Cu_4Pr$ | –27.8 | –34.6 |
| $Cu_2Pr$ | –43.6 | –43.6 |
| CuPr | –46.7 | –42.6 |

**Note:** Standard states are liquid Cu and liquid Pr.
(**a**) From [83Nie].

The decomposition temperatures of the various intermediate phases were determined from the temperature variation of the integral molar Gibbs energy of the phases. In all instances, the decomposition temperatures were found to be above their respective formation temperatures, indicating that these phases are quite stable at all points below their formation temperatures.

The enthalpy data from the present modeling are compared in Table 6 with the enthalpies of formation derived with the semi-empirical model of Miedema [80Mie, 83Nie]. The Miedema estimates are closely comparable to the calculated results. The maximum deviation between the two results, observed for $Cu_4Pr$, is only ~7 kJ/mol, which is not large considering the approximations involved in the two approaches.

### Cited References


***34Can:** G. Canneri, "Alloys of Praseodymium and Copper," *Metall. Ital., 26,* 869-871 (1934) in Italian. (Equi Diagram, Thermo; Experimental; #)

**61Dwi:** A.E. Dwight, "Factors Controlling the Occurrence of Laves Phases and $AB_5$ Compounds among Transition Elements," *Trans. ASM, 53,* 479-500 (1961). (Equi Diagram, Crys Structure; Experimental)

**61Gsc:** K.A. Gschneidner, Jr., *Rare Earth Alloys,* D. Van Nostrand Co., Inc., Princeton, NJ, 158 (1961). (Equi

Diagram, Crys Structure; Compilation; #)

**63Sto:** A.R. Storm and K.E. Benson, "Lanthanide-Copper Intermetallic Compounds having the $CeCu_2$ and $AlB_2$ Structure," *Acta Crystallogr., 16,* 701-702 (1963). (Crys Structure; Experimental)

**65Dwi:** A.E. Dwight, R.A. Conner, Jr., and J.W. Downey, "Crystal Structures of Compounds of the Rare Earths with Cu, Ag, Au, and Ga," Proc. 5th Rare Earth Res. Conf., Aug 30-Sept 1, 1965, Ames, IA, *5,* 35-44 (1965). (Crys Structure; Experimental)

**65Wal:** R.E. Walline and W.E. Wallace, "Magnetic and Structural Characteristics of Lanthanide-Copper Compounds," *J. Chem. Phys., 42*(2), 604-607 (1965). (Crys Structure; Experimental)

**70Bus:** K.H.J. Buschow and A.S. van der Goot, "The Crystal Structure of Some Copper Compounds of the Type $RCu_6$," *J. Less-Common Met., 20,* 309-313 (1970). (Crys Structure; Experimental)

**71Bus:** K.H.J. Buschow and A.S. van der Goot, "Composition and Crystal Structure of Hexagonal Cu-Rich Rare Earth-Copper Compounds," *Acta Crystallogr. B, 27*(6) 1085-1088 (1971). (Crys Structure; Experimental)

**74Wun:** M. Wun and N.E. Phillips, "Low-Temperature Heat Capacity of $PrCu_2$," *Phys. Lett. A, 50*(3), 195-196 (1974). (Thermo; Experimental)

**75And:** K. Andres, E. Bucher, P.H. Schmidt, J.P. Maita, and S. Darack, "Nuclear-Induced Ferromagnetism below 50 mK in the Van Vlack Paramagnet $PrCu_5$," *Phys. Rev. B, 11*(11), 4364-4372 (1975). (Crys Structure; Experimental)

**78Bea:** B.J. Beaudry and K.A. Gschneidner, Jr., "Preparation and Basic Properties of the Rare-Earth Metals," in *Handbook on the Physics and Chemistry of Rare-Earths,* Vol. 1-*Metals,* K. A. Gschneidner, Jr. and L. Eyring, Ed., North-Holland Physics Publishing Co., Amsterdam, 173-232 (1978). (Equi Diagram; Compilation)

**79Pop:** I. Pop, E. Rus, M. Coldea, and O. Pop, "Knight Shift and Magnetic Susceptibilities of Intermetallic Compounds $PrCu_4$ and $PrCu_5$," *Phys. Status Solidi (a), 54,* 365-368 (1979). (Crys Structure; Experimental)

**80Mie:** A.R. Miedema, P.F. de Chatel, and F.R. de Boer, "Cohesion in Alloys - Fundamentals of a Semi-Empirical Method," *Physica B, 100,* 1-28 (1980). (Thermo; Theory)

**81And:** A. Andreeff, E.A. Goremychkin, H. Greismann, L.P. Kaun, B. Lippold, W. Matz, O.D. Chistyakov, E.M. Savitskii, and P.G. Ivanitskii, "The Crystal Field in the Hexagonal Compound $PrCu_5$," *Phys. Status Solidi (b), 108,* 261-267 (1981). (Crys Structure; Experimental)

**81Blo:** J.M. Bloch, D. Shaltiel, and D. Davidov, "Preparation and Study of New Intermetallic Compounds with the $NaZn_{13}$ Structure: $LaCu_{13}$, $PrCu_{13}$," *J. Less-Common Metals, 79,* 323-327 (1981). (Crys Structure; Experimental)

**82Gsc:** K.A. Gschneidner, Jr. and F.W. Calderwood, "Critical Evaluation of Binary Rare Earth Phase Diagrams," Report IS-RIC-PR-4, Rare-Earth Information Center, Iowa State University, Ames, IA (1982). (Equi Diagram, Crys Structure; Compilation)

**83Cha:** M.W. Chase, "Heats of Transition of the Elements," *Bull. Alloy Phase Diagrams, 4*(1), 123-124 (1983). (Thermo; Compilation)

**83Gsc:** K.A. Gschneidner, Jr. and F.W. Calderwood, "Critical Evaluation of Binary Rare Earth Phase Diagrams," Report IS-RIC-PR-7, Rare-Earth Information Center, Iowa State University, Ames, IA (1983). (Equi Diagram, Crys tructure; Compilation)

**83Kwa:** K. Kwasnitza, B. Barbisch, and F. Hulliger, "Metallic Materials for Superconductor Stabilization with Very High Specific Heat and Good Thermal Conductivity," *Cryogenics, 12,* 649-652 (1983). (Thermo; Experimental)

**83Nie:** A.K. Niessen, F.R. de Boer, R. Boom, P.F. de Chatel, W.C.M. Mattens, and A.R. Miedema, "Model Predictions for the Enthalpy of Formation of Transition Metal Alloys II," *Calphad, 7*(1), 51-70 (1983). (Thermo; Theory)

**86Gsc1:** K.A. Gschneidner, Jr., private communication (1986).

**86Gsc2:** K.A. Gschneidner, Jr. and F.W. Calderwood, "Intra Rare Earth Binary Alloys: Phase Relationships, Lattice Parameters and Systematics," in *Handbook on the Physics and Chemistry of Rare Earths,* Vol. 8, K.A. Gschneidner, Jr. and L. Eyring, Ed., North-Holland Physics Publishing Co., Amsterdam, 1-161 (1986). (Equi Diagram, Crys Structure; Compilation)

*Indicates key paper.

#Indicates presence of a phase diagram.

Cu-Pr evaluation contributed by **P.R. Subramanian,** Materials Science Division, Universal Energy Systems, Incorporated, 4401 Dayton, OH 45435 and **D.E. Laughlin,** Department of Metallurgical Engineering and Materials Science, Carnegie Mellon University, Pittsburgh, PA 15213.
Work was supported by the International Copper Research Association, Inc. (INCRA) and the Department of Energy through the Joint Program on Critical Compilation of Physical and Chemical Data coordinated through the Office of Standard Reference Data, National Bureau of Standards. The authors wish to thank Dr. K.A. Gschneidner, Jr., Director, and F.W. Calderwood, Rare-earth Information Center, Ames Laboratory, Iowa State University, Ames, IA, for providing part of the bibliographic search and the computer program for the critical evaluation of crystallographic data. The authors would also like to thank Dr. D.J. Chakrabarti for his assistance with some of the computer programs, and Dr. H. Okamoto for valuable suggestions. Literature searched through 1985. Professor Laughlin is the ASM/NBS Data Program Category Editor for binary copper alloys.

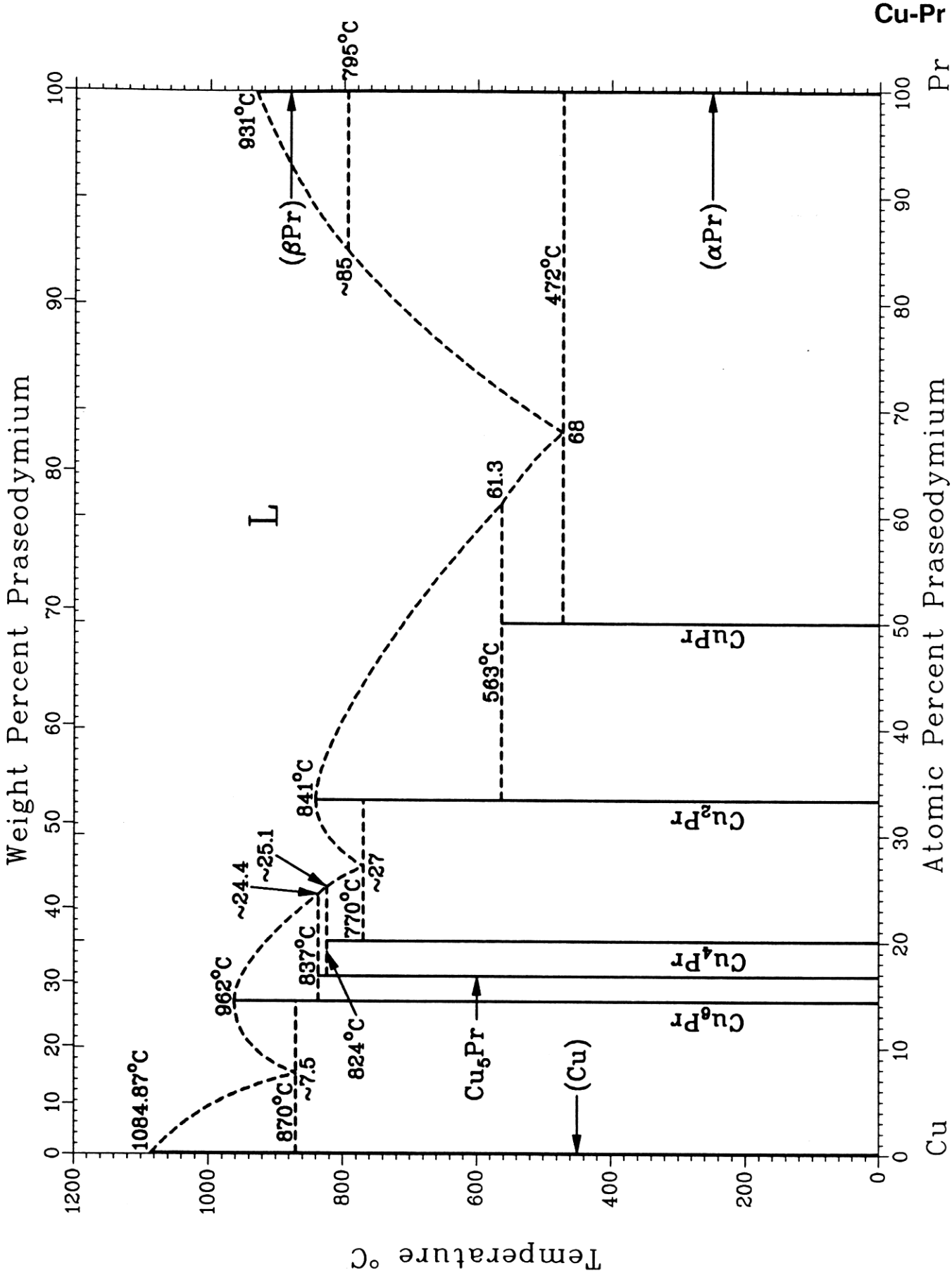


**P.R. Subramanian and D.E. Laughlin**

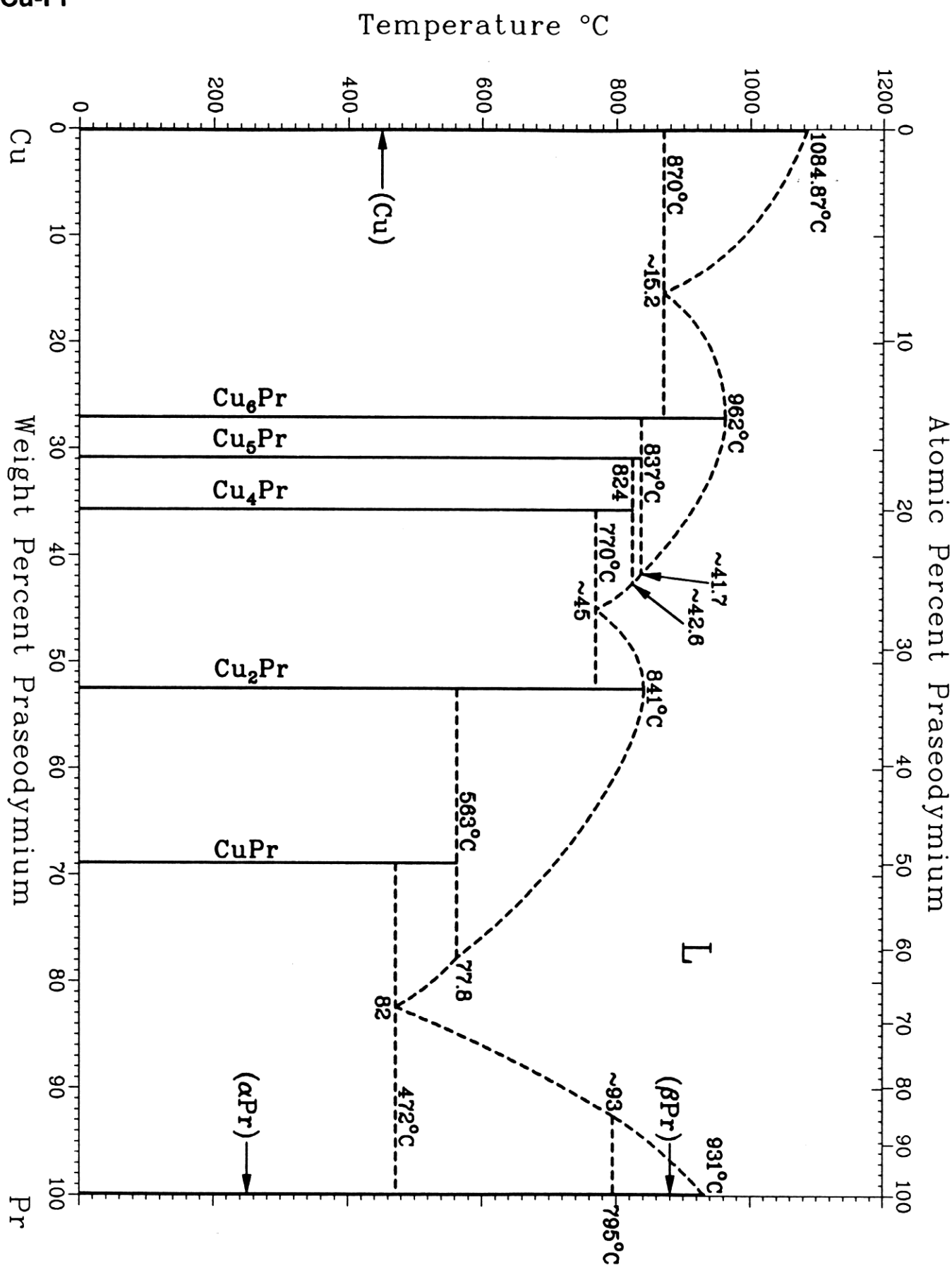


P.R. Subramanian and D.E. Laughlin